J. Membrane Biol. 75, 45–56 (1983)

The Journal of
Membrane Biology

Monolayer Black Membranes from Bipolar Lipids of Archaebacteria and Their Temperature-Induced Structural Changes

Alessandra Gliozzi*, Ranieri Rolandi**, Mario De Rosa*** and Agata Gambacorta***

Istituto di Cibernetica e Biofisica, CNR, Camogli, 16032 Italy*, Istituto di Scienze Fisiche dell'Università di Genova, 16132 Italy**, and Istituto per la Chimica di Molecole di Interesse Biologico, Arco Felice (NA), 80072 Italy***

Summary. The membrane of *Caldariella acidophila,* an extreme thermophilic archaebacterium, is characterized by unusual bipolar complex lipids. They consist of two nonequivalent polar heads, linked by a C_{40} alkylic component. The molecular organization of these lipids in the plasma membrane is still a matter of study. In this paper, we present current-voltage measurements on artificial bipolar lipid membranes, indicating that molecules are indeed organized as a covalently bound bilayer, in which each molecule is completely stretched and spans its entire thickness. Furthermore, conformational transitions of these artificial membranes (which could be formed only above 70° C from a lipid/squalene dispersion) are analyzed in the 80 to 15° C temperature range. Abrupt variations in capacitance and valinomycin-induced conductance seem to indicate the occurrence of at least two structural changes. Measurements are also extended to different solvent systems. Results are consistent with the picture of a monolayer bipolar lipid membrane in which few solvent molecules align themselves parallel to the lipophilic chains. The amount of solvent as well as the temperature at which conformational transitions occur, depend on the solvent system in which the lipid is dispersed.

Key Words bipolar lipid membranes · archaebacteria membranes · conformational transitions

Introduction

A recent phylogenetic analysis based upon ribosomal RNA sequence [3, 36, 41, 42], RNA polymerases [43], translation system [21], tRNAs [16], 5SrRNA [26], cell walls [9, 18, 19, 44], and lipids [11, 12, 20, 24, 25, 27, 35] reveals that living systems can be classified into three different lines: eubacteria, eukaryotes and archaebacteria. This comparative molecular analysis also reveals an ancient divergence, and now archaebacteria appear to be as different from eubacteria as they are from eukaryotes.

Some features (e.g., the absence of a nuclear membrane and organelles, the low DNA content, and their dimensions) indicate that archaebacteria are prokaryotic cells.

The evolutive line of archaebacteria consists of methane-generating bacteria (methanogens), a group of salt-tolerant bacteria (halophiles), and some acid-tolerant thermophiles [40].

Archaebacteria thrive under conditions of very high temperature, extreme pH, saturated salt solution or strict anaerobiosis, which would in general kill or strongly limit development of other living organisms.

In view of the key role played by the membranes in the survival of archaebacteria under environmental stresses, studies have been carried out to identify the structure and biogenetic origin of membrane lipids. All the lipids of archaebacteria are based on ether linkages, obtained by condensation of glycerol or more complex polyols with two isoprenoid alcohols at 20, 25 or 40 carbon atoms.

Because of their unusual structure, archaebacteria lipids can be regarded as a specific taxonomic marker of this new line of evolution.

Figure 1 shows the basic structural elements from which the complex lipids, present in the different groups or archaebacteria, derive.

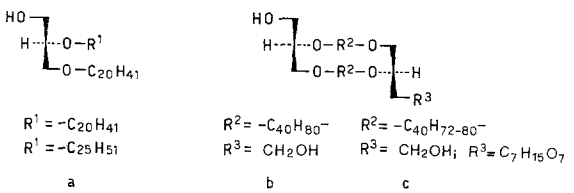

Fig. 1. Complex membrane lipids of archaebacteria stem from the interactions of the free hydroxylic functions of these structures with sugars, polyols, phosphoric residue, etc. Halophilic archaebacteria possess lipids based on diethers (*a*); methanogenic archaebacteria have lipids based on diethers (*a*) ($R^1 = -C_{20}H_{41}$), and on tetraethers (*b*); thermophilic archaebacteria have lipids based on tetraethers (*c*). Lipids used in this work have $R^3 = C_7H_{15}O_7$

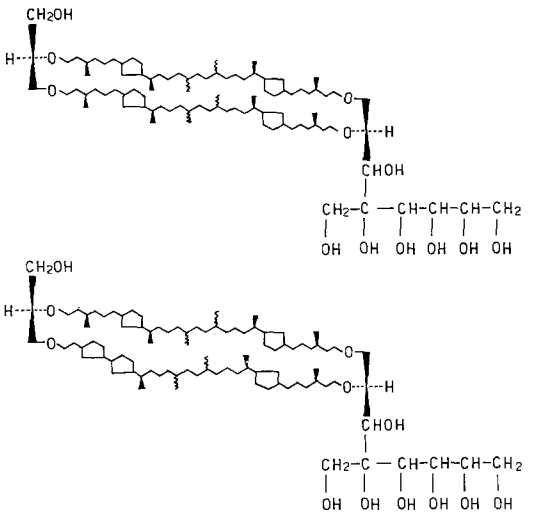

Fig. 2. Fine structures of main components of glycerol-dialkyl-nonitol tetraether mixture from *Caldariella acidophila* lipids. The other molecular species differ in the degree of cyclization of C_{40} chains, which have up to four cyclopentane rings

The unusual structure of archaebacteria lipids raises the problem of the organization of this type of molecules in the membrane; such a problem is particularly interesting in the case of thermophilic archaebacteria, whose membrane lipids are all based on macrocyclic tetraethers (Fig. 1*c*), which have an unusual molecular architecture. In fact, while classic lipids are monopolar amphipatic molecules, which have only one polar head and one aliphatic component attached to it, the complex lipids of thermophilic archaebacteria are bipolar amphipatic molecules characterized by the presence of two nonequivalent polar heads, linked by a C_{40} alkylic component, which is practically twice the length of the components of classic lipids.

Two different molecular arrangements can be assumed by bipolar lipids in the bilayer: either a covalently bound bilayer, in which each molecule is completely stretched and spans its entire thickness, or a bilayer in which the two polar heads, being anchored to the same side of the membrane-solution interface, induce a bending of the hydrophobic chains. In the remainder of this paper, we shall call the latter arrangement a "U-shaped" configuration of lipids. Indirect evidence concerning the structure and dimensions of the lipids themselves, the absence of a preferential fracture plane in the middle of the lipid layer [25], and the extreme rigidity of the thermophilic archaebacteria membrane [25], suggests that the membrane lipids are organized as a covalently bound bilayer. Further evidence has been obtained by experiments performed on bipolar lipids from the plasma membrane of *Caldariella acidophila,* an extremely thermoacidophilic archaebacterium [8, 29], both in the intact cells of the microorganism by the selective labeling of the external polar head [12], and on artificial planar bipolar lipid membranes [13–15]. In this paper, we present evidence of this arrangement, deduced from the current-voltage behavior of an artificial membrane prepared with the tetraethers shown in Fig. 1*c* ($R^2 = -C_{40}H_{72-80}-$; $R^3 = C_7H_5O_7$). Such a behavior, obtained on a membrane which has been forced to undertake an asymmetrical configuration, indicates that bipolar lipids are indeed organized as a covalently bound bilayer.

The potentiality of this new artificial membrane seems to be essentially related to its stability over a wide range of temperatures. Therefore, it appears to be the ideal model for studying phenomena in which lipid phase transitions play a major role. Accordingly, electrochemical measures, such as capacitance and valinomycin-induced conductance, have been obtained in the melting and freezing temperature ranges.

Results are compared with previous data on phase transitions in usual lipid bilayers [2, 5, 23, 37]. The analysis is extended to bipolar lipid membranes dispersed in various solvent systems.

These measurements suggest a picture of a monolayer bipolar lipid membrane, which is fluid in the range of physiological tolerance ($\simeq$91 to 68° C) and undergoes several structural changes as temperature decreases. Few solvent molecules are likely to be located parallel to the lipophilic chains, the exact amount depending on the solvent system in which the lipid is dispersed. A comparative study between these membranes and a bilayer structure may provide a deeper insight into the role of the Van der Waals interactions between apposed hydrophobic tails in the mid-plane of the bilayer.

Materials and Methods

The experiments were performed using a crude mixture of glycerol-dialkyl-nonitol tetraethers (GDNT), characterized by two nonequivalent polar heads ($R^2 = -C_{40}H_{72-80}-$; $R^3 = C_7H_{15}O_7$, *see* Fig. 1*c*) from *Caldariella acidophila* grown at 85° C in the usual way [8].

Extraction of complex lipids, their hydrolysis and purification of glycerol-dialkyl-nonitol tetraethers have been described in a previous work [7]. Fine structures of the main component of the tetraether mixture are presented in Fig. 2.

Calorimetric measurements were performed on the dry sample using a differential scanning calorimeter (Mettler TA 3000).

Black membranes were formed while operating above 70° C with a 25 mg/ml dispersion of GDNT in squalene. Membranes could also be formed at a lower temperature by adding chloroform or butanol. However, no membrane formation could be obtained below approximately 40° C. Membranes were made with the Rudin and Mueller technique on a circular hole, usually 0.6 mm in diameter. The cell had optically flat windows at both ends, and it was held in a copper thermostat. Temperature was monitored with a thermistor. The area of the membrane was determined photographically, using transmitted light. The estimated error was of the order of 0.3%.

The signal was applied to the membrane via a voltage-clamp circuit, according to the usual two-electrode configuration using an LF 356 (National Semiconductor) operational amplifier. Ag/AgCl electrodes were employed for applying and recording potentials. They were either 2 mm in diameter and 3 cm long or plate electrodes with a 7 cm^2 exposed area. No difference was found between both electrode sets. Particular care was taken to preserve the electrodes; e.g., they were kept under short-circuit in the dark. Potential difference between each pair of electrodes was controlled before and after each series of measurements. It never exceeded 0.5 mV.

Membrane capacitances were measured at 500 Hz ($V_{AC}(\max) = \pm 50$ mV) with a precision (0.1%) AC impedance bridge. Extrapolation to zero potential was found to introduce negligible corrections in the capacitance values. Current-voltage characteristics were determined by applying a single impulse of a triangle wave (usually 10^{-2} Hz and 200 mV peak to peak). The signal was recorded on a Bryans 29000 X-Y recorder. To get asymmetric current-voltage curves, a continuous potential (either 30 or 50 mV) was applied to the membrane for 10 to 15 min before each series of measurements. Such a procedure was also found to stabilize the value of the capacitance.

Membrane conductance was determined using a square wave of 20 mV peak to peak at 0.1 Hz. A current-voltage converter based on an operational amplifier (LH 0052 National Semiconductor) was used to monitor the signal on an HP 7402 oscillographic recorder. The sensitivity of the measurements was dependent on the magnitude of the currents, owing to the presence of noise at the smallest currents (of the order of few pA), and of fluctuations in particular ranges of temperature. Usually it was around 5%. When measurements were performed in the presence of valinomycin, this molecule was added to the external solution from ethanolic stock solution (3×10^{-3} M). Valinomycin was purchased from Calbiochem (Los Angeles, Calif.), and squalene from Sigma Chemical Co. (St.Louis, Mo.).

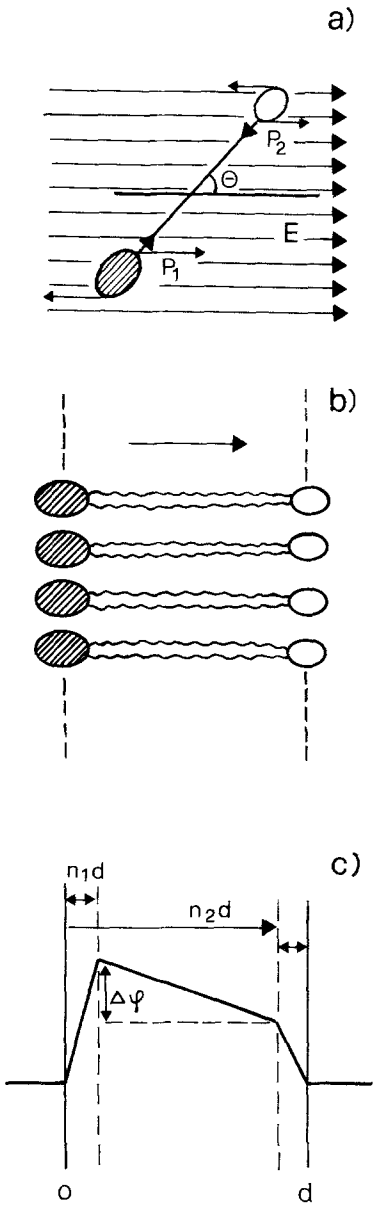

Fig. 3. *a)* Schematic representation of a bipolar lipid molecule assuming a stretched configuration in an external field. *b)* Sketch indicating the orientation of molecules in the membrane. *c)* Schematic representation of the energy potential barrier

Results

Current-Voltage Measurements

In this section, we report on experiments aimed to get information on the molecular organization of lipids in the membrane. The rationale for this set of experiments is based on the following considerations. The two polar heads of the lipid molecules are quite different (*see* Fig. 2). At one end there is a glycerol, while at the other end there is a ramified polyvalent alcohol, with nine hydroxyles. If the molecule assumes a stretched configuration, it can be schematized as a rod, with two different electrical dipole moments at their ends. This rod will orient itself in an external electric field according to the minimum energy value, which corresponds to the angle $\Theta = 0$ (*see* Fig. 3*a*). Thus, upon application of an external field, one expects to find a large part of the membrane molecules oriented, in order to reach the minimum energy value (*see* Fig. 3*b*). Such orientation will lead to unequal potential profiles, at the membrane-solution interfaces. The two different potential profiles will in turn induce an internal potential difference $\Delta\varphi$, as shown in Fig. 3*c*.

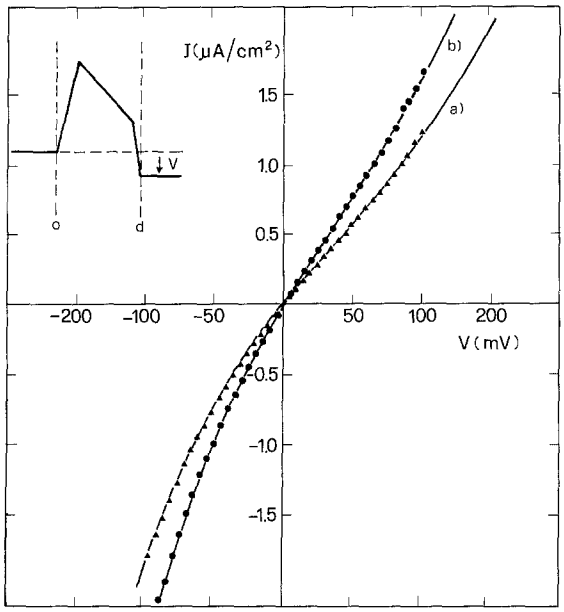

Fig. 4. Current-voltage curve in the presence of valinomycin: *a)* the membrane has been oriented by applying 50 mV for 15 min; *b)* the same membrane 10 min after the first recording. The continuous line is the theoretical curve, deduced from Eq. (1), while points and triangles are reported from current-voltage measurements, after having subtracted the capacitive current. Frequency of the triangular wave $\gamma = 10^{-2}$ Hz. Ionic solution: 10^{-1} M KCl. $T = 77°$ C. The insert illustrates the potential barrier considered and the conventional sign of the applied potential

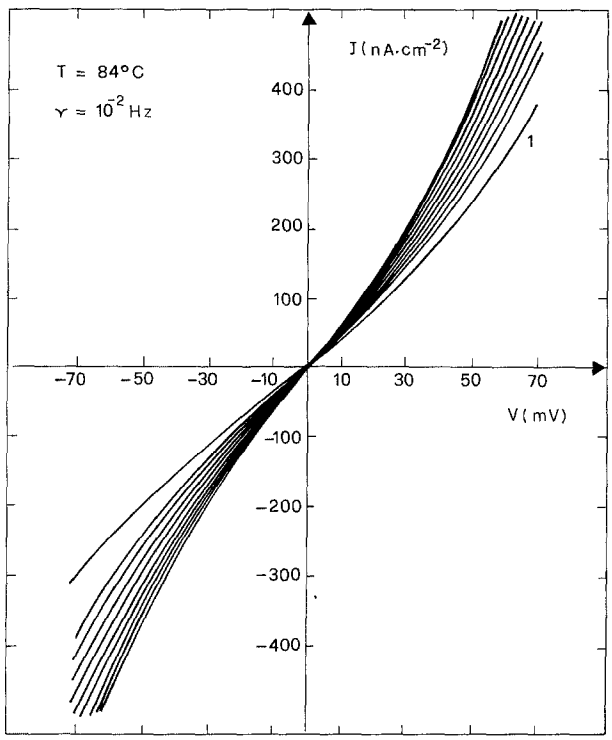

Fig. 5. Successive current-voltage runs performed at a frequency $\gamma = 10^{-2}$ Hz (except for curve number 1, for which $\gamma = 0.5$ 10^{-2} Hz) on an unmodified membrane. The membrane was oriented with a -50 mV potential (opposite sign of Fig. 4). Ionic solution: KCl 10^{-1} M. $T = 84°$ C

The conductance of such a membrane is thus expected to be asymmetrical, both because of the different energy barriers and of the presence of an internal electric field. To monitor such asymmetry, current-voltage characteristics (I–V) induced by valinomycin were recorded. The ionic solution concentration was 10^{-1} M KCl. The results are shown in Fig. 4. The points represent the experimental values obtained from the continuous I–V measurements, while the continuous line is the fit to the points performed by use of Eq. (1) with the following parameters: $\Delta\varphi$, the internal potential difference, n_1 and $1\text{-}n_2$, the fractional distance from the corner (*see* Fig. 3*c*). The insert in Fig. 4 shows a schematic representation of the energy barriers considered, and the Appendix gives the details of derivation of Eq. (1).

The experiments shown in Fig. 4*a* refer to a membrane oriented with an external potential of 50 mV lasting about 15 min at $T = 77°$ C. The fitting to the experimental points gives $\Delta\varphi = 40$ mV and $n_1 = 1\text{-}n_2 = n = 0.14$. A second set of measurements was performed by applying an external potential of 30 mV to the membrane. In this case, the fitting gives $\Delta\varphi = 25$ mV and the same value of n.

Control experiments were also performed by carefully washing the cell (to avoid artifacts due to previous orientation of molecules in the torus) and by applying the electric field in the opposite direction. The reverse behavior of the curve was indeed found. If any external field is removed and the same measurement is repeated after a certain time lag, the current-voltage curve turns out to be slightly changed. Figure 4*b* shows the current-voltage curve performed on the same membrane as in Fig. 4*a* after a time lag of 10 min. The asymmetry is clearly less pronounced and the value of $\Delta\varphi$ is equal to 38 mV.[1] This behavior indicates that the molecules, which have been forced to assume an asymmetrical organization of their polar heads in the membrane, tend towards a random distribution with time. Such a tendency can be better observed in the absence of valinomycin. In fact, in this case, the rate of symmetrization is higher, as shown in Fig. 5. Here, except for the first curve,

[1] This difference, although small, is still significant. In fact if a value of $\Delta\varphi = 40$ mV were used to fit the points of Fig. 4*b*, one had obtained systematically lower currents. For instance at $V = 100$ mV the corresponding shift is $\Delta J = 0.06$ μA/cm², which is about three times larger than the sensitivity of the measurements.

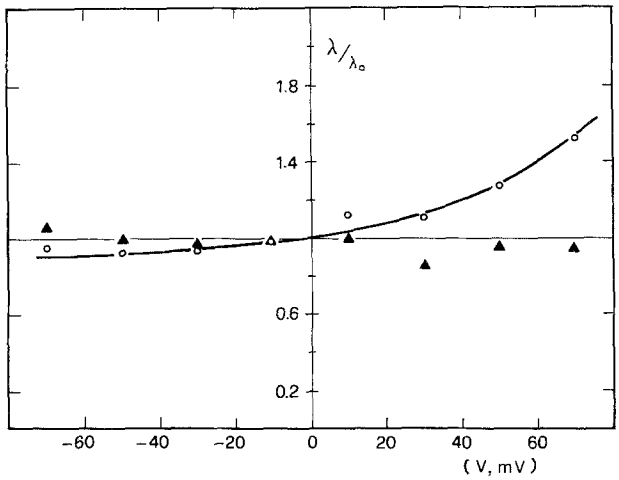

Fig. 6. The normalized cord conductance, λ/λ_o, of unmodified membrane is plotted against the applied voltage. Each point is the mean value over three different membranes. Nonconditioned membranes (▲); membranes conditioned with −50 mV for 15 min (o); λ_o is the cord conductance at −10 mV. $T>$ 65° C; ionic solution: KCl 10^{-1} M

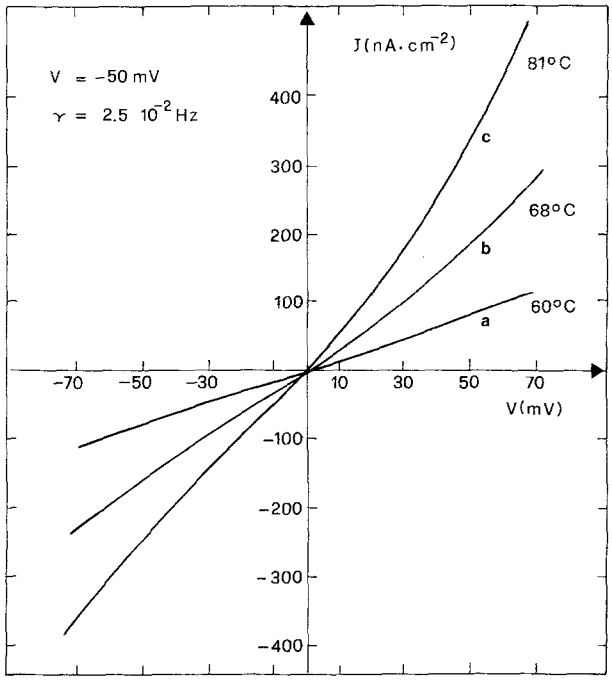

Fig. 7. Current-voltage runs performed at the indicated temperatures on an unmodified membrane. Before each run, a potential of −50 mV was applied to the membrane for 10 min. Ionic solution: KCl 10^{-1} M. Other conditions as indicated

for which the frequency was halved, the current-voltage curve was repeated at a frequency $\nu = 10^{-2}$ Hz.

One might suspect that the current-voltage measurements could affect the membrane orientation. To minimize such an effect, measurements were performed by applying the triangle voltage wave with an increasing positive or negative voltage, according to the sign of the field employed to orient the molecules. Moreover, the overall I–V excursion lasted a much shorter time (usually 10^2 s) than that needed to get appreciable orientation ($\simeq$10 to 15 min). With these precautions, the curves obtained during the increasing and the decreasing runs of the triangle wave differed only in the capacitive currents. In the results shown in Figs. 4, 5 and 6, the capacitive currents have been subtracted.

Notice that in all the curves of Figs. 4 and 5 the "zero current conductance" has a tendency to increase in successive runs, after having applied positive and negative potentials of the order of 100 mV. This phenomenon, observed also in non-oriented membranes, may be related to the formation of oriented domains, connected by less ordered regions of higher aspecific permeability.

A further set of control experiments was performed by measuring current-voltage characteristics prior to the voltage conditioning of the membrane, both in the presence and in the absence of valinomycin. In most experiments no asymmetry was observed. In some cases, however, while operating at high temperature (>75° C) and in the absence of valinomycin, an asymmetry was exhibited by the membrane. However, no preferential occurrence of a higher current on one of the two sides of the membrane was observed. Figure 6 illustrates such a point, giving the mean value of the normalized conductance over different membranes prior to and after the voltage conditioning.

It is of primary importance to clarify the influence of temperature on the fluidity of the membrane and, consequently, on the possibility of orienting the bipolar molecules. To this aim, the following set of experiments were performed. Membranes were formed at the usual temperature, cooled to 50° C and successively warmed again. During the warming phase, an external potential of −50 mV was applied. Under these conditions, no orientation was obtained up to 60° C, as shown by the current-voltage curve in Fig. 7*a*. By contrast, a clear asymmetry in the current-voltage behavior can be observed at 68° C and, even more pronounced, at 81° C (Figs. 7*b* and *c*). The above results indicate therefore that the hydrophobic chains are still partially frozen at 60° C, severely limiting the molecular orientation induced by the electric field, while the larger fluidity found above 68° C allows such a phenomenon. The above findings have therefore suggested the systematic investigation of the temperature-induced structural changes undergone by the lipid membrane; they will be reported in the remainder of this work.

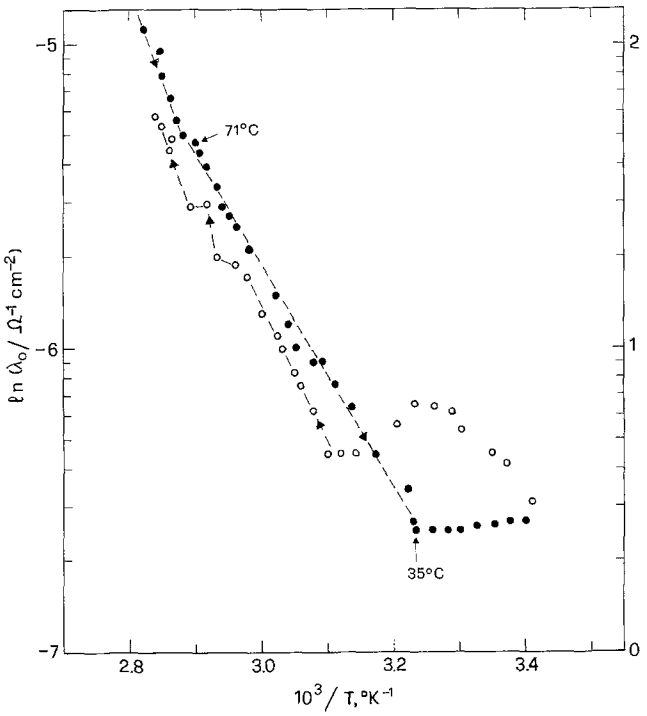

Fig. 8. The logarithm of "zero current" conductance, λ_o, induced by valinomycin is plotted against the reciprocal of absolute temperature, $1/T$, for a GDNT/squalene membrane. Notice the break in the straight-lines at the indicated temperature values. Valinomycin concentration: 5×10^{-8} M. Ionic solution: 10^{-1} M KCl

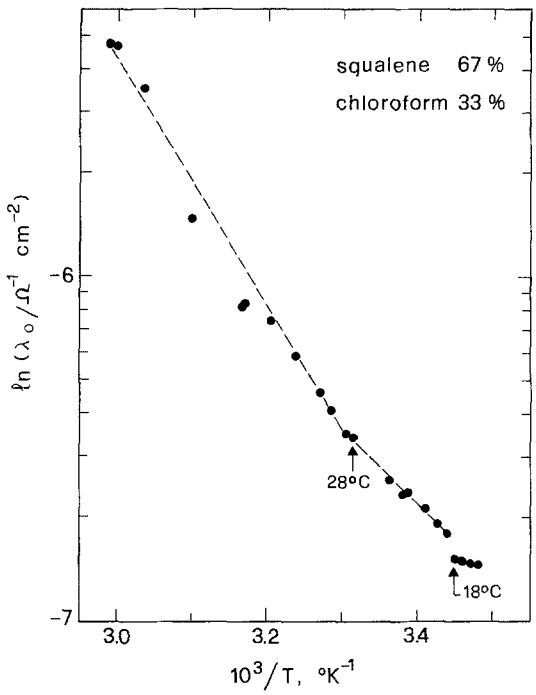

Fig. 9. The logarithm of "zero current" conductance, λ_o, is plotted against the reciprocal of absolute temperature, $1/T$, for a GDNT/squalene-chloroform membrane at the indicated percentages. Measurements were performed by decreasing the temperature at a rate of about 1° C/min. The break in the straight-lines and the corresponding temperature values are indicated. The point where the conductance levels off might simply correspond to the reaching of the bare membrane conductance. Valinomycin concentration: 5×10^{-8} M. Ionic concentration: 10^{-1} M KCl

Effects of Structural Changes in Lipids on Carrier-Mediated Ionic Transport

In several cases, valinomycin was shown to act as a probe of phase transition, as well as of secondary structural changes in lipids [5, 22, 23]. In spite of the very unusual lipid structure, valinomycin is still acting as a carrier in the present system [13]. Information on membrane structural changes, induced by lowering temperature, could thus be obtained by inserting valinomycin and measuring the membrane conductance. To bring this trend into clearer evidence, data are presented on a single membrane. However, the results on different membranes are qualitatively identical. The conductance logarithm has been plotted in Fig. 8 versus the reciprocal of the absolute temperature, $1/T$. The straight line indicates an exponential conductance behavior as a function of $1/T$, as expected for an Arrhenius plot. Below 71° C, the activation energy is about 17 kcal/mol, and this value was found to be quite reproducible on different membranes. Below 35° C, conductance does not vary any more and its value is within the bare membrane conductance range. This fact indicates that valinomycin is almost immobilized, in agreement with previous findings on usual lipid bilayers [5, 23]. The warming curve shows almost the same behavior, with a hysteresis loop.

The same measurements were repeated on a membrane formed from GDNT dispersed in squalene and chloroform (2:1 by volume). A similar trend is observed, as Fig. 9 shows. However, the break occurs at lower temperature (around 28 and 18° C). Valynomicin is not immobilized even below 28° C. The break at 18° C might correspond to some structural change in the membrane; in any case, it is the point where valinomycin-induced conductance is likely to be of the same order as that of the bare membrane.

Effects of Structural Changes in Lipids on Specific Capacitance

Membrane capacitance C_s was measured independently by lowering the temperature at the rate of 1° C/min. Data on a single membrane are described below. Results were not mediated from different experiments, since values of specific geometric capacitance in the case of membranes formed from the same solvent rarely varied more than 1%.

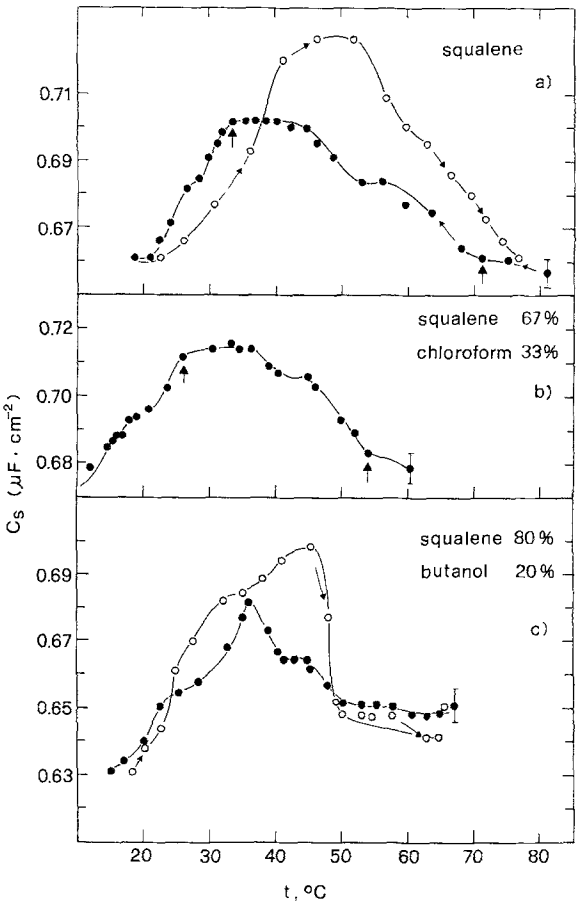

Fig. 10. Specific geometric capacitance is plotted aginst temperature for a membrane from a GDNT dispersion in the three different solvent systems. The approximate precision of the measurements (±0.4%) is indicated. The arrows indicate the points where major changes in the slope of $C_S(t)$ are observed, and correspond, in the cases *a)* and *b)*, to breaks in the logarithm of conductance (*cf.* Figs. 8 and 9). The continuous curves have no theoretical meaning. (●) Pattern of decreasing temperature; (○) Pattern of increasing temperature Ionic solution: KCl 10^{-1} M

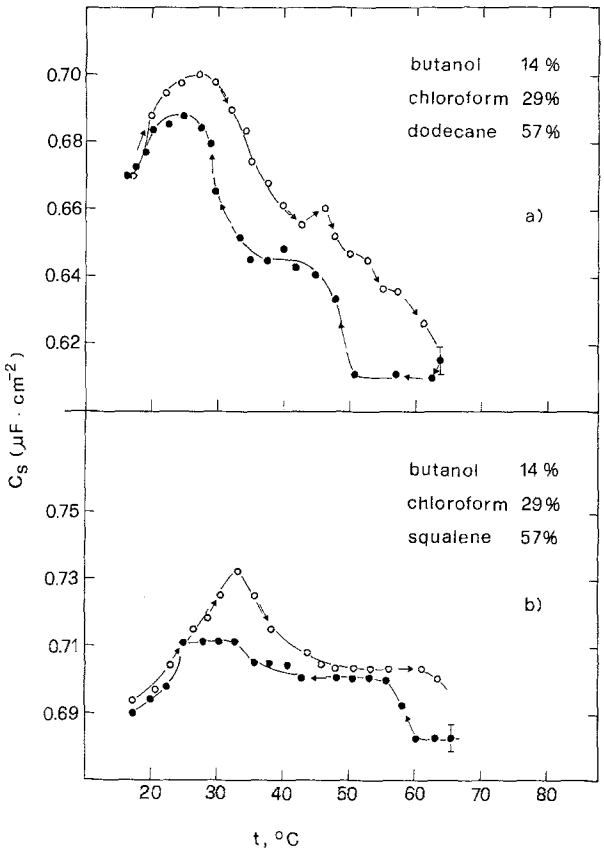

Fig. 11. Specific geometric capacitance is plotted against temperature for a membrane from a GDNT dispersion in two different solvent systems. Notice that the abrupt changes in the slope of $C_S(t)$ for the dodecane membrane. Changes in the slope of $C_S(t)$ are also observed in curve (*b*). (●) Cooling curve; (○) Warming curve. Ionic solution: NaCl 10^{-1} M

Figures 10 and 11 show capacitance values plotted as a function of temperature for membranes formed from GDNT dispersed in various solvent systems. A comparative analysis of these data is very useful as it suggests the interpretation of the curves, which will be dealt with in the Discussion section.

A feature common to all the curves is a bell-shaped configuration. The overall capacitance variation is around 6%, except for the dodecane curve (Fig. 11*a*) where a 12% variation occurs. The maximum capacitance value and the changes in the slope of $C_S(t)$ occur, however, at temperatures which are peculiar to any solvent system. The warming and cooling curves are quite similar, except for a hysteresis. In the warming curve, irregularities are less pronounced.

While performing the measurements, the membrane does not seem to lose solvent (especially chloroform or butanol) to a noticeable extent. In fact, in almost all the experiments, the initial and final capacitance values in the cooling and in the warming curves, respectively, do coincide.

Measurements in Figs. 10*a* and *b* refer to membranes in the presence of valinomycin. As far as capacitance values are concerned, no significant difference was found in the presence or absence of valinomycin at the aqueous concentrations employed ($C_0 \simeq 5 \times 10^{-8}$ M).

Figure 10*a* refers to a GDNT membrane dispersed in squalene. The arrows indicate the temperatures at which major changes in the slope of $C_S(t)$ occur. It appears that such values correspond to the indicated breaks of the Arrhenius plot in

Fig. 8, performed on the same membrane, in the same cooling-warming cycle.

Figure 10*b* shows data on a GDNT membrane dispersed in a mixture of squalene and chloroform. These data should be compared with those relevant to the corresponding valinomycin-induced conductance, as shown in Fig. 9. As in the previous case the drastic change in the slope of $C_S(t)$ occurring around 28° C, corresponds to the indicated break of Fig. 9.

Figure 10*c* refers to a GDNT membrane dispersed in squalene and butanol. Also in this case, drastic changes in the slope of $C_S(t)$ can be observed.

Figures 11*a* and *b* compare the behaviors of two membranes formed from a dodecane and a squalene dispersion, respectively. Addition of chloroform and butanol at the indicated percentages was performed in order to get long-lasting membranes. In fact, films from pure dodecane dispersions were quite unstable. In these latter solvent systems, major differences are observed. Not only are the changes in slope shifted with respect to each other but also the overall capacitance variation is different. The main reason for such a difference is that, at high temperatures, capacitance is noticeably lower in membranes from dodecane-chloroform-butanol dispersions than in all the other cases. Nonetheless, the maximum capacitance value is almost the same ($C_S = 0.697 \pm 0.013\ \mu F/cm^2$) for all the solvent systems so far analyzed. A higher excursion of capacitances is thus observed.

Discussion

Asymmetric Energy Barriers Induced by an Electric Field

Figures 4, 5 and 6 show an asymmetry in the current-voltage behavior of a membrane separating two identical solutions. It clearly reflects an asymmetry in the membrane structure itself, which can be exhibited by a covalently bound bilayer having two different polar heads, but not by a membrane with a U-shaped configuration of molecules. This finding is by far the most important one and constitutes the strongest evidence, indicating that molecules are indeed organized as a bipolar lipid monolayer. Stretched chains in equilibrium with some molecules, assuming a U-shaped configuration, are, however, not excluded by the present set of experiments.

Results presented in Fig. 6 exclude the existence of intrinsic asymmetries of the measuring apparatus. One might suspect that polarization during the membrane conditioning could cause the observed I–V relation asymmetries. However, in this case the degree of asymmetry should correlate with the conductance of the membrane. Comparison of Figs. 4, 5 and 7 indicates that this is not the case.

Data in Fig. 4 have been fitted by Eq. (1) which has been derived by assuming that the process of complex formation occurs sufficiently rapidly so that it can be considered to be at equilibrium relative to the movement of the complexed carrier. This assumption implies that our system is in the realm of behaviors which has been termed "equilibrium domain" [6]. Such an assumption is consistent with several data on the GDNT/squalene membrane, such as those relevant to the hyperbolic behavior of the current-voltage curve, to the lack or shift of saturation in the linear behavior of conductance versus ionic concentration (as compared with a glycerol-monooleate (GMO) membrane [13]. The goodness of the fit shown in Fig. 4 further supports this series of arguments.

Notice that in the current-voltage curve in Fig. 4, the current is higher on the side of negative potentials. This kind of asymmetry cannot be accounted for by electrode polarization artifacts, which would affect the potential difference between the two solutions but not the barrier shape across the membrane-solution interface (*cf.* Eq. 1). By contrast the shape of the I–V curve is consistent with the shape of the barrier shown in the inset of Fig. 4. This barrier shape is that expected to result if the applied conditioning potential caused a reorientation of the lipids so that their dipole moments were parallel to the direction of the conditioning field.

The value of the fractional distance from the corner, $n = 14\%$, indicates that the diffusion barrier extends across 70% of the membrane interior, in agreement with previous findings [22] for a variety of carriers and ion systems.

When the electric field is removed, current-voltage curves tend to exhibit a symmetrical behavior, as Figs. 4*b* and 5 show. This indicates that the membrane, which has been forced to assume an asymmetrical configuration, tends towards a random distribution of lipid polar heads. Two possible mechanisms might explain this behavior. First, the molecules could undergo a flip-flop movement, which is almost hindered in either natural [4] or artificial [17, 32] normal bilayers. Such a flip-flop movement is not even expected to occur in *Caldariella acidophila* plasma membrane *in vivo* since the polar heads of complex lipids are much

bigger, having anchored other functional groups, such as phosphoric residues, sugars or polyols [14]. Alternatively, a diffusional exchange with the torus molecules, enhanced by the higher temperature, relative to a typical BLM, might explain such a behavior. Further work is, however, required to get a better understanding of this phenomenon.

Phase Transitions as Deduced from Combined Capacitance and Conductance Measurements

The data presented here indicate that planar bipolar lipid membranes, formed from GDNT and various solvent systems, undergo significant structural changes with temperature.

Calorimetric studies, performed on the dry sample, show two phase transitions around 70 and 34° C.[2] These points correspond to breaks in the $\ln \lambda_o(1/T)$ curve and to changes in the slope of $C_S(t)$ for a squalene/GDNT membrane. We shall first analyze this system. Two further data indicate that around 70° C there is a partial freezing of the chains. Firstly, membranes could not be formed below 70° C without addition of chloroform or butanol to the GDNT/squalene dispersion. Secondly, data in Fig. 7 indicate that orientation of the membrane dipoles induced by an electric field does not occur below 68° C. This set of data suggests that conformational transitions also occur in these planar bilayer membranes.

It may be of interest to compare the observed transition temperatures T_c with those of a saturated diacyl phosphatidylcholine, in the hydrated liquid crystalline state. For a C_{22} chain, $T_c = 75°$ C, while for a C_{18} chain, $T_c = 58°$ C (the number of carbon atoms includes the ester group). For a hydrocarbon crystal $C_{20}H_{42}$, $T_c = 36.7°$ C [34].

Membranes formed from mixtures of GDNT/squalene (or dodecane), in the presence of chloroform and/or butanol, do present also discontinuity points in conductance and capacitance, as Figs. 9, 10 and 11 show. However, the transition points are shifted towards lower values. Besides the main changes discussed so far there are in the temperature-dependent conductance and capacitance curves minor breaks. However, in conductance measurements although out of the instrumental precision, these breaks are within the range of fluctuations which have often been observed, while in capacitance measurements they are not completely out of the experimental precision, indicated in Figs. 10 and 11.

Previous work on glycerol-monooleate/*n*-alkanes membranes [37] has shown that changes in the capacitance slope correspond to a phase transition in the membrane. Two structural changes were observed by White, who suggested that they might be due to transition and pretransition. Alternatively, the two changes might represent, according to White, the beginning and the end of a single broad transition or the result of a complex phase diagram of a two-component mixture.

In the present case a more exact interpretation of data requires additional experimental effort. Separation and purification of the tetraether mixture (Fig. 1*c*, $R^2 = -C_{40}H_{72-80}-$; $R^3 = C_7H_{15}O_7$) is almost completed, and measurements are being repeated on the single components.

Capacitance-Temperature Behavior

The results shown in Figs. 10 and 11 demonstrate that specific capacitance depends, within a 10% variation, on the solvent system in which the lipid is dispersed. This suggests that small amounts of solvent are present in the membrane. They are likely to be located parallel to the C_{40} lipophilic chains, as found for long *n*-alkanes (greater than 12 carbons) in lipid-alkane vesicles [28]. Solvent molecules may affect the value of C_S due to two combined actions. They may stretch the chains, thus increasing the membrane thickness d; at the same time, they may reduce the area per molecule at the interfaces. As a consequence, the dielectric coefficient ε_r, would decrease, since the number of polarizable molecules per unit volume would decrease. Both factors would contribute in increasing C_S ($C_S = \varepsilon_o \varepsilon_r / d$). As an example, let us analyze capacitance values at 62° C, shown in Figs. 11*a* and *b*. The only difference between the two experiments lies in the presence of dodecane instead of squalene. Capacitance in dodecane is 0.620 μF/cm², while in squalene it is 0.683 μF/cm². This 10% variation is likely to be ascribed to the higher amount of solvent in the dodecane-containing membrane.

Comparison of data in Figs. 10 and 11 shows that the mean value of capacitance at its maximum is (0.697 ± 0.013) μF/cm². Therefore it is independent, within the experimental error, of the initial composition of the membrane. It follows that, at

[2] Calorimetric measurements performed on the dry sample of GDNT showed two broad transitions peaking around 34 and 70° C. Their apparent enthalpy production, ΔH, was equal to 820 cal/mol and 760 cal/mol, respectively. Such a low value of enthalpy is likely to be due to incomplete structural changes in the entire sample, at the indicated temperatures, owing to the heterogeneity of its composition. Furthermore, these values of ΔH may be affected by deviations of up to 50% due to the small enthalpy production and to the broadness of the peaks.

the corresponding values of temperature, the membrane is likely to be almost solvent-free.

The overall capacitance behavior suggests the following model. Upon cooling the system, the partial freezing of the chains induces the formation of solid and fluid domains. Lateral phase separation with solvent exclusion into microlenses or into torus is thus expected to occur, as described by White [37] for glycerol monooleate/*n*-alkanes membranes. The increase in capacitance derives from the combined effect of a decrease in length and an increase in dielectric constant. It should be observed, however, that the overall capacitance variation is 6% for all the solvent systems, with the only exception of dodecane. This means that if only the thickness of the membrane would vary, there would be a decrease of 1.5 Å, while if the thickness were constant and only the dielectric coefficient, ε_r, could vary, a change from $\varepsilon_r = 2.1$ to $\varepsilon_r = 2.2$ would occur. These changes should be doubled in the case of dodecane membranes, where a 12% variation in capacitance occurs.

The falling part of the curve has thus to be compared with a solvent-free bilayer, cooled below its phase transition. The capacitance behavior is similar to that described by Boheim et al. [5] for a 1-stearoyl-3-myristoyl-glycero-2-phosphocholine membrane formed by the Montal and Mueller method. The decrease in capacitance corresponds to a variation in length due to stretching of the chains upon freezing. This corresponds to a thickness change in the membrane hydrocarbon core of about 1.5 Å for all the experimental data in Figs. 10 and 11.

Capacitance-Voltage Behavior

The picture presented above allows an insight into previously measured compressibility data [14]. A proportionality constant α relates the capacitance at zero potential, $C(0)$, to the capacitance at a potential V, $C(V)$, according to the relationship:

$$C(V) = C(0)\,(1 + \alpha V^2).$$

The coefficient α at 72° C in GDNT/squalene membranes is $(0.16 \pm 0.06) V^{-2}$ and $(0.40 \pm 0.05) V^{-2}$ in GDNT/dodecane. These values of α are about one order of magnitude higher than those for a GMO/squalene membrane ($\alpha \simeq 0.03) V^{-2}$ [39] or solvent-free GMO bilayers ($\alpha = 0.036 \pm 0.002\ V^{-2}$) [1]. They are, however, more than one order of magnitude lower than a GMO/dodecane membrane ($\alpha = 8.5 \pm 0.6\ V^{-2}$). By contrast, at 42° C in GDNT/squalene films $\alpha < 0.05\ V^{-2}$, i.e., of the same order as in solvent-free bilayers. The different values of α seem to be related to the different solvent content inside the membrane. Data presented in this work show, however, that solvent molecules are likely to align themselves parallel to the lipid biphytanyl chains, in contrast with usual bilayers with short *n*-alkanes (smaller than 14 carbons), where they are mainly located in the midplane region [38]. Application of an electric field induces squeeze-out of solvent in the present system, as in usual lipid bilayers. The mechanism leading to an increase in capacitance would be the one previously described, which acts on the membrane, when cooling the system from 70 to 40° C. In particular, the different values of α for GDNT/squalene and GDNT/dodecane would simply reflect the different solvent amounts in the film. On the other hand, the fact that the value of α at 42° C is of the same order of magnitude as in solvent-free bilayers further indicates that the membrane is indeed solvent-free at such temperature values.

Conductance-Temperature Behavior in the Presence of Valinomycin

The Arrhenius plot of zero-current conductance induced by valinomycin in a GDNT/squalene membrane, illustrated in Fig. 8, gives an activation energy, ΔG^*, which is about 17 kcal/mol below 71° C. Stark et al. [33] have found, for a dierucoyllecithin bilayer, in the presence of valinomycin, $\Delta G^* = 17$ kcal/mol, a value within the same range. If we consider the temperature-induced change in the fluidity coefficient of a saturated paraffinic or naphthenic mineral oil [30], we find an activation energy which is of the same order of magnitude (8 to 13 kcal/mol). This comparison suggests that the presently measured activation energy mainly reflects both the change in the fluidity of the hydrocarbon core and a presumably smaller decrease in the valinomycin-potassium concentration in the membrane (due to a decrease in the valinomycin-K^+ partition coefficient, or in the equilibrium constant of complex formation). At $T = 35°$ C valinomycin is immobilized, indicating a completely frozen state of the membrane. Such a behavior has already been observed in usual bilayers [5, 23]. The relative maximum that is noticed in the warming curve is likely to be ascribed to an increase of the bare membrane conductance. Such an increase may be related to phenomena similar to fluctuations which have been observed in usual lipids near the phase transition [2, 5]. It might reflect a contribution of unspecific conduction through the membrane in regions joining inhomogeneous structures.

The effect of chloroform on the conductance conferred upon a membrane by valinomycin is illustrated in Fig. 9. Two values of activation energies, within the same range as the previous ones, are observed. Also in these membranes there is a simultaneous change in conductance and capacitance, around 28° C. Thus the effect of chloroform would be that of lowering the temperature of the main transition.

Final Remarks

The results reported here further support the hypothesis of a monolayer organization of bipolar lipids in the membranes of thermophilic archaebacteria. This finding is very important from an evolutionary point of view, in that this new model of molecular membrane architecture is the first example of an alternative topologic solution in a structure that, until now, has appeared to have remained basically unchanged from the most simple prokaryotes up to humans.

It is appealing to speculate on the possible physiological role of such a covalently bound bilayer. In the plasma membrane of *Caldariella acidophila,* this organization may accomplish a double task . Firstly, it confers stability to the membrane, subject to awful environmental stresses. Secondly, it may constitute a barrier against the diffusion of hydrogen ions into the cell. In fact, the cell membrane is subject to a tremendous proton gradient (the pH of the external environment is $\simeq 1.5$, while the cytoplasmic one is $\simeq 6.5$). The mechanism of action would be the following. The polar head including the polyvalent alcohol nonitol is linked with sugars; these, in turn, are directed towards the outside of the cell. The plasma membrane is therefore asymmetrical in its lipid structure. Consequently, a higher dipole potential barrier, hindering proton permeation even through possible hydrophilic patterns, will develop at the external interface. Clearly, a U-shaped configuration of molecules would not have given such a barrier.

We thank M. Robello and E. Gaggero for designing the capacitance bridge, G. Paoli for helpful observations on valinomycin measurements and W. Stuehmer for reading the manuscript.

This work was partially supported by the Consiglio Nazionale delle Ricerche, with a grant of the "Programma finalizzato Chimica Fine Secondaria" in the framework "Membrane e Processi di Membrana."

Appendix

The Nernst-Planck equation applied to a charged carrier moving through an asymmetrical trapezoidal barrier has already been derived in an explicit form by Schoch et al. [31]. Such a derivation is suitable for the present system, allowing equilibrium of the interfacial reactions. The only significant difference lies in the shape of the barrier, which in the present system is due to a different dipole field instead of a surface charge asymmetry. However, even if two different slopes were assumed for the rising part of the trapezoidal barrier (as suggested for the present system, as a sum of the dipole and of the Born potentials), the final current-voltage relationship would remain unchanged. Since no significant modifications are introduced, we omit reporting the detailed derivation. The resulting current-voltage curve is:

$$I = K \frac{\Delta\varphi + (n_2 - n_1) V}{n_2 - n_1} \quad \frac{1 - \exp(aV)}{\exp a(\Delta\varphi + n_2 V) - \exp(an_1 V)} \qquad (1)$$

where K is a factor which is considered constant for a given membrane and includes the diffusion coefficient of the complex, the equilibrium constant for the interfacial reactions, the partition coefficient of the carrier, the ion and carrier concentrations in the aqueous solution; a is defined as zF/RT (where the symbols have their usual meanings); n_1, n_2 and $\Delta\varphi$ describe the trapezoidal barrier (*see* Fig. 3*c*), and V is the applied voltage.

References

1. Alvarez, O., Latorre, R. 1978. Voltage-dependent capacitance in lipid bilayers made from monolayers. *Biophys. J.* **21**:1–17
2. Antonov, V.F., Petrov, V.V., Molnar, A.A., Prevoditelev, D.A., Ivanov, A.S. 1980. The appearance of single-ionic channels in unmodified lipid bilayer membrane at the phase transition temperature. *Nature (London)* **283**:585–586
3. Balch, W.E., Fox, G.E., Magrum, L.J., Woese, C.R., Wolfe, R.S. 1979. Methanogens: Reevaluation of a unique biological group. *Microbiol. Rev.* **43**:260–296
4. Bergelson, L.D., Barsukov, L.I. 1977. Topological asymmetry of phospholipids in membranes. *Science* **197**:224–230
5. Boheim, G., Hanke, W., Eibl, H. 1980. Lipid phase transition in planar bilayer membrane and its effect on carrier- and pore-mediated ion transport. *Proc. Natl. Acad. Sci. USA* **77**:3403–3407
6. Ciani, S.M., Eisenman, G., Laprade, R., Szabo, G. 1973. Theoretical analysis of carrier-mediated electrical properties of bilayer membranes. *In:* Membranes. A Series of Advances. G. Eisenman, editor. Vol. 2, pp. 61–177. Marcel Dekker, New York
7. De Rosa, M., De Rosa, S., Gambacorta, A., Bu'Lock, J.D. 1980. Structure of calditol, a new branched-chain nonitol, and of the derived tetraether lipids in thermoacidophilic archaebacteria of the *Caldariella* group. *Phytochemistry* **19**:249–254
8. De Rosa, M., Gambacorta, A. Bu'Lock, J.D. 1975. Extremely thermophilic acidophilic bacteria convergent with *Sulfolobus acidocaldarius*. *J. Gen. Microbiol.* **86**:156–164
9. De Rosa, M., Gambacorta, A., Millonig, G., Bu'Lock, J.D. 1974. Convergent characters of extremely thermophilic acidophilic bacteria. *Experientia* **30**:866–868
10. De Rosa, M., Gambacorta, A., Nicolaus, B. 1983. A new membrane model, in thermophilic archaebacteria, based on bipolar ether lipids. J. Membr. Sci. (*in press*)
11. De Rosa, M., Gambacorta, A., Nicolaus, B., Bu'Lock, J.D. 1980. Complex lipids of *Caldariella acidophila,* a thermoacidophile archaebacterium. *Phytochemistry* **19**:821–825
12. De Rosa, M., Gambacorta, A., Nicolaus, B., Ross, H.H.M., Grant, W.D., Bu'Lock, J.D. 1982. An asymmetric archaebacterial diether lipid from alkaliphilic halophiles. *J. Gen. Microbiol.* **128**:343–348

13. Gliozzi, A., Paoli, G., Rolandi, R., De Rosa, M., Gambacorta, A. 1982. Structure and transport properties of artificial bipolar lipid membranes. *J. Bioelectrochem. Bioenerg.* **9**:591–601
14. Gliozzi, A., Rolandi, R., De Rosa, M., Gambacorta, A. 1982. Artificial black membranes from bipolar lipids of thermophilic archaebacteria. *Biophys. J.* **37**:563–566
15. Gliozzi, A., Rolandi, R., De Rosa, M., Gambacorta, A., Nicolaus, B. 1982. Membrane models of archaebacteria. *In:* Transport in Biomembranes. R. Antolini, A. Gliozzi and A. Gorio, editors. pp. 39–48. Raven Press, New York
16. Gupta, R., Woese, C.R. 1980. Unusual modification patterns in the transfer ribonucleic acids of archaebacteria. *Curr. Microbiol.* **4**:245–249
17. Hall, J.E. 1981. Voltage-dependent lipid flip-flop induced by alamethicin. *Biophys. J.* **33**:373–381
18. Kandler, O., Hippe, H. 1977. Lack of peptidoglycan in the cell walls of *Methanosarcina barkeri*. *Arch. Microbiol.* **113**:57–60
19. Kandler, O., König, H. 1978. Chemical composition of the peptidoglycan-free cell walls of methanogenic bacteria. *Arch. Microbiol.* **118**:141–152
20. Kates, M., Kushwaha, S.C. 1978. Biochemistry of the lipids of extremely halophilic bacteria. *In:* Energetics and Structure of Halophilic Microroganisms. S.R. Caplan and M. Ginzburg, editors. pp. 461–479. Elsevier, North Holland Biomedical Press, Amsterdam
21. Kessel, M., Klink, F. 1980. Archaebacterial elongation factor in ADP-ribosylated by diphteria toxin. *Nature (London)* **287**:250–251
22. Krasne, S., Eisenman, G. 1976. Influence of molecular variations of ionophore and lipid on the selective ion permeability of membranes: I. Tetranactin and the methylation of nonactin-type carriers. *J. Membrane Biol.* **30**:1–44
23. Krasne, S., Eisenman, G., Szabo, G. 1971. Freezing and melting of bilayers and the mode of action of nonactin, valinomycin and gramicidin. *Science* **174**:412–415
24. Kushwaha, S.C., Kates, M., Sprott, G.D., Smith, I.C.P. 1981. Novel complex polar lipids from the methanogenic archaebacterium *Methanospirillum hungatei*. *Science* **211**:1163–1164
25. Langworthy, T.A. 1978. Membranes and lipids of extremely thermoacidphilic microorganisms. *In:* Biochemistry of Thermophily. S.M. Friedman, editor. pp. 11–30. Academic Press, New York
26. Luehrsen, K.R., Nicholson, D.E., Eubanks, D.C., Fox, G.E. 1981. An archaebacterial 5SrRNA contains a long insertion seque *London)* **293**:755–756
27. Makula, R.A., Singer, M.E. 1978. Ether-containing lipids of methanogenic bacteria. *Biochem. Biophys. Res. Commun.* **82**:716–722
28. McIntosh, T.J., Simon, S.A., MacDonald, R.C. 1980. The organization of *n*-alkanes in lipid bilayers. *Biochim. Biophys. Acta* **597**:445–463
29. Millonig, G., De Rosa, M., Gambacorta, A., Bu'Lock, J.D. 1975. Ultrastructure of an extremely thermophilic acidophilic microorganism. *J. Gen. Microbiol.* **86**:165–173
30. Naal, M.J., editor. 1973. Tribology Handbook, B2. Butterworths, London
31. Schoch, P., Sargent, D.F., Schwyzer, R. 1979. Capacitance and conductance as tools for the measurement of asymmetric surface potentials and energy barriers of lipid bilayer membranes. *J. Membrane Biol.* **46**:71–89
32. Sherwood, D., Montal, M. 1975. Transmembrane lipid migration in planar asymmetric bilayer membranes. *Biophys. J.* **15**:417–434
33. Stark, G., Benz, R., Pohl, G.W., Janko, K. 1972. Valinomycin as a probe for the study of structural changes of black lipid membranes. *Biochim. Biophys. Acta* **266**:603–612
34. Tanford, C. 1973. The Hydrophobic Effect: Formation of Micelles and Biological Membranes. John Wiley & Sons, London
35. Tornabene, T.G., Langworthy, T.A. 1979. Diphytanyl and dibiphytanyl glycerol ether lipids of methanogenic archaebacteria. *Science* **203**:51–53
36. Tu, J., Prangishvilli, D., Huber, H., Wildgruber, G., Zillig, W., Stetter, K.O. 1982. Taxonomic relations between archaebacteria including 6 novel genera examined by cross hybridizations of DNAs and 16S rRNAs. *J. Mol. Evol.* **18**:109–114
37. White, S.H. 1975. Phase transitions in planar bilayer membranes. *Biophys. J.* **15**:95–117
38. White, S.H. 1977. A study of the physical chemistry of planar bilayer membranes using high precision measurements of sepcific capacitance. *Ann. N.Y. Acad. Sci.* **303**:243–252
39. White, S.H. 1978. Formation of "solvent-free" black lipid bilayer membranes from glycerol monooleate dispersed in squalene. *Biophys. J.* **23**:337–347
40. Woese, C.R. 1981. Archaebacteria. *Sci. Am.* **244**:94–107
41. Woese, C.R., Fox, G.E. 1977. Phylogenetic structure of the prokaryotic domain: The primary kingdoms. *Proc. Natl. Acad. Sci. USA* **74**:5088–5090
42. Woese, C.R., Magrum, L.J., Fox, G.E. 1978. Archaebacteria. *J. Mol. Evol.* **11**:245–252
43. Zillig, W., Schnabel, R., Tu, J., Stetter, K.O. 1982. The phylogeny of archaebacteria, including novel anaerobic thermoacidphiles in the light of RNA polymerase structure. *Naturwissenschaften* **69**:197–204
44. Zillig, W., Stetter, K.O., Schäfer, W., Janekovic, D., Wunderl, S., Holz, I., Palm, P. 1981. Thermoproteales: A novel type of extremely thermoacidophilic anaerobic archaebacteria isolated from Icelandic solfataras. *Zentralbl. Bakteriol. Parasitenkd. Infektionskr. Hyg. Abt. 1. Orig.* **C2**:205–227

Received 1 September 1982; revised 16 December 1982